The Method of Instant Amplification of the MCG&MEG Signals

R. Sklyar

Verchratskogo st. 15-1, Lviv 79010 Ukraine, sklyar@tsp.lviv.ua

ABSTRACT

The method of magnetocardiography and magnetoencephalography signals on-site amplification by an electromagnetic transistor, with a simultaneous filtration of movement interferences is advanced. A current trend in these type of diagnostics is a portable and wearable magnetometer systems. Which have, at the same time, high signal processing and signal-to-noise ratio parameter data characteristics. The ferroelectric (FE) or ferroelectromagnetic (FEM) transistor is combined with a superconducting magnetometer for distributed amplification of the biosignals. The interferences from the natural movements of the body is proposed to be eleminated by the filters, which are specific for each part of a wide frequency range. The designed sensors are arranged in space arrays for investigation of the biosignals of the different levels of precision with a defined informational capabilities.

Keywords: ferroelectromagnetic, superconducting induction magnetometer, interferences, arrays, sensing area

1 INTRODUCTION. STATE-OF-THE-ART MCG&MEG

In order to obtain high-quality ECG signals, an ultralow-power low noise ASIC (60 nV/√Hz) with an accoupled instrumentation amplifier is used [1]. The amplifier rejects the common-mode signals coupled to human body, and also filters the differential DC voltage generated between two biopotential electrodes in order to prevent saturation of the circuit, and minimizes the CMRR degradation under electrode impedance mismatch. This allows a non-stop wireless acquisition of an ECG signal on cost of its quality even under severe energy deficit, where the full-quality signal acquisition cannot be maintained.

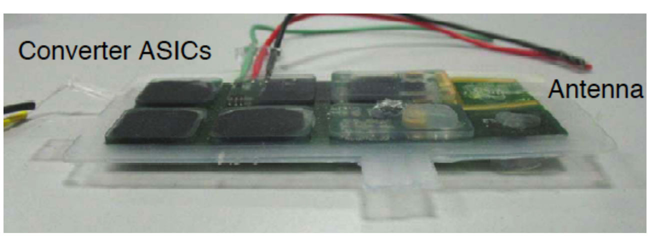

Figure 1: Encapsulated flexible electronics module.

The electronics module is integrated in a twosided flex circuit, Fig. 1. The circuit is divided into quasirigid islands with dense components alternated with empty flexible zones. This gives a limited amount of flexibility to the circuit and makes it compatible with embedding in clothes and with laundry (very high accelerations). The batteries at the bottom of the circuit also serve as placeholders to keep the substrate a minimum distance of about 2 mm away from the skin. This improves the antenna performance characteristics as compared to direct contact of the module with the skin.

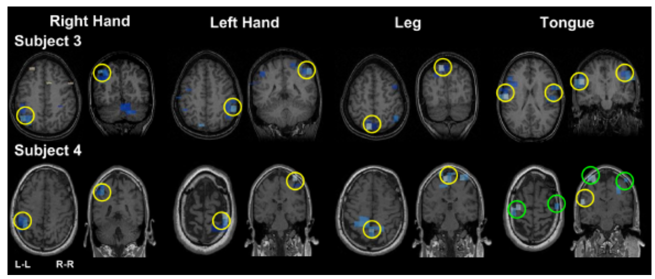

Figure 2: SAM image: activation in the corresponding motor areas associated with the intention to move.

Magnetocardiography (MCG) is a noninvasive method of detecting the cardiac magnetic fields (MFs) above the body surface using DC superconducting quantum interference devices (SQUIDs). Also most SQUIDs are incorporated into whole-head systems for magnetoencephalography (MEG)- the detection of MFs produced by brain (Fig. 2). MEG provides direct information about the dynamics of evoked and spontaneous neural activity, and better spatial resolution so that we might accurately decode more brain information/minds, and eventually it might be possible to actually “read” human mind instead of indirect control of brain rhythmic activity. Synthetic aperture magnetometry (SAM) has been employed for signal processing and better signal-to noise ratio (SNR) [2].

2 DESCRIPTION OF THE MEASURING METHOD WITH A FILTERING ABILITY

A carbon nanotubes field-effect transistor (CNT FET) with a high-temperature superconducting channel was introduced into the nerve fibre or brain tissue for transducing their signals in both directions. On the basis of depicted transducer a combined processor for the natural and artificial information was advanced [3]. The design and mathematical description of an biomagnetic array of electromagnetic transistors/memristors (EMTMs) which are ordered in the memristor architecture was proposed [4]. It was shown that the noise can be effectively cancelled by synthetic higher-order gradiometers. EMTM is combined with a superconducting magnetometer for distributed amplification of the biosignals (Fig. 3).

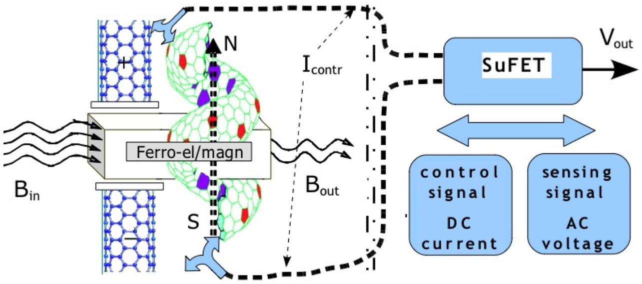

Figure 3: A shematic diagram of EMTM based head sensor which is controlled/preamplified by a SuFET device and is subject to natural vibrations of a body.

The superconducting FET (SuFET) is incorporated into a wide-band MF sensor device in order to acquire an ultimate sensitivity. A further step should be employing an active core in a control/pickup coil (CPC) for additional processing of MCG & MEG, as necessary for the diagnostics. The EM sensors are surface CPCs, which are used in regular configuration where CPCs with a small distance between each other are positioned within the helmet type surface to pick up the local signals within the place of interest.

A current trend in such diagnostics are portable and wearable magnetometer systems which have, in the same time, high signal processing and signal-to-noise ratio parameter data characteristics. That is why on-site amplification of MCG&MEG signals by a close body device with a simultaneous filtration of movement interferences is high on the agenda. This device incorporates the advantages of CNT FET's superconducting ability with suitability of the nanowires for a printed electronic process. The acquired system has a room-temperature working mode without the necessity of rigid fastening.

2.1 The Device for a Transducing Process

The control signal I_{contr} which creates MF B in CPC's core during a direct mode of SuFET operation (Fig. 3) according to a law of an EM induction as:

$$B = I_{contr} L / \mu_{eff} NS \quad (1)$$

where S is an average area of PC's cross-section, N- total turn number, L- inductance of PC, μ_{eff}- effective relative permeability of a FE or FEM core.

The output sensing voltage of MCG&MEG signals is acquired by functioning of SuFET in a reverse mode:

$$V_{out} = BS\omega K_{SuFET} \mu_0 \mu \quad (2)$$

where $\mu_0 = 4\pi \cdot 10^{-7}$- permeability of free space, (henry/meter), ω- frequency in radians, K_{SuFET}- internal parameters of SuFET.

2.2 The Circuit's Elements and Spurious Values Which are Forming an Output Signal

The advanced device of Fig. 3 can be shown by an equivalent circuit in Fig. 4 with the introduced spurious values (SV): C_g and M_W. A core of PC is put into a working point by a current of SuFET's channel I_{contr} which creates an electric field (EF) in a plate E_{contr} or MF H in a coil W_{contr}. The pulsations of I_{contr} are smoothing by a capatitance C_g. An output current on PC I_{sign} is amplifying by FET into an output voltage U_{out}.

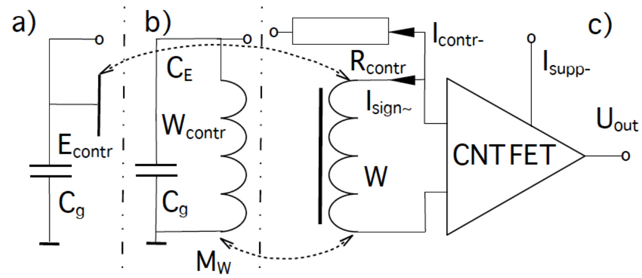

Figure 4: Equivalent circuit of EM amplifier: a) and b) are electric and magnetic field control sections respectively; c) supply and sensing CNT FET with a nanowired pickup.

The AC signal processing circuit is shown in Fig.3. CNT are surrounding a core in order to apply E_{contr}. H_{contr} is created by additional turns which are wound under both the CNT and windings W of PC. The inductance of PC is increased by its mutual inductance with windings of W_{contr} and C_g- by a capacitance between the plate and PC.

In such arrangement the EM control values are calculated as follows:

$$E_{contr} = \frac{U_0}{R}\left(\ln\frac{2d}{R}\right)^{-1}; \quad H_{contr} = -\frac{LW_{contr}}{\mu_0 \mu_{eff} SW^2} \quad (3)$$

where R is the radius of CNT and d is the distance from CNT to a core.

Shown in Fig. 4 spurious values are being calculated as:

$$C_m = \frac{4\pi^3 \varepsilon \varepsilon_0 l}{\left(\ln\left(\frac{16l}{a}\right)\right)^2 + \frac{\pi^2}{12}} \quad (4)$$

$$M_W = \sum_{k_1=1}^{\omega} \sum_{k_2=1}^{\omega} \int_0^{\pi} \frac{\mu_0 r_1 r_2 \cos\varphi d\varphi}{\sqrt{\left((k_1 - k_2)h\right)^2 + r_1^2 + r_2^2 - 2r_1 r_2 \cos\varphi}} \quad (5)$$

where $\varepsilon_0 = 10^{-9}/36$ F/m, ε is an electric permeability of the composing material; 2a and 2l are diameter of CNT and their length respectively.

In Eq. (5) r_1 and r_2 are the diameters of turns W and W_{contr} respectively with equal winding steps h, and k_1 and k_2 are sequential numbers of their windings.

After calculating the variables C_g and M_W we can define a transfer function of the circuit in Fig. 4 as:

$$G = \frac{U_{out}}{H} = \frac{\omega KM}{\sqrt{\left(1 + \frac{R}{R_{ch}} - \frac{x_L}{x_C}\right)^2 + \left(\frac{x_L}{R_{ch}} + \frac{R}{x_C}\right)^2}} \quad (6)$$

where $x_L=\omega L+M_L$, $x_C=(1/C_M+1/C_g)/\omega$.

If conditions $R/R_{ch}\approx 1$; $\omega\approx 100$ are true, we have a simplified value:

$$G=\omega KM \quad (7)$$

A number of CNT which are surrounding a FM rod for applying control EF can be calculated according to the angle β of a respective segment:

$$N_{max}=360°/\beta \quad (8)$$

where $\beta=2\mathrm{ArcSin}(2a/2r_3)$, r_3- an imaginary radius which includes a circle of CNT.

Taking into account the technological ability for attaching real CNT, their number can be estimated as:

$$N_{real}=N_{max}/2 \quad (9)$$

As a result we can find the summarized EF from N_{real} CNT around a FM rod according to:

$$\Sigma E=\sqrt{N_{real}}\cdot E_0 \quad (10)$$

2.3 The Filtering Principle for LF

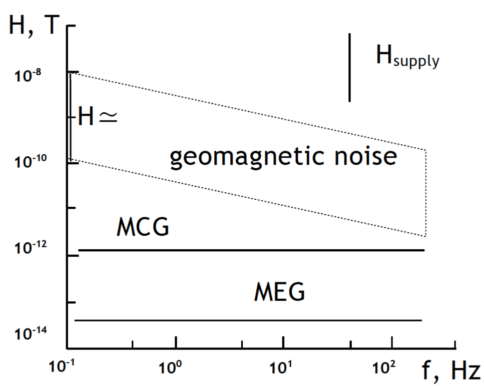

Figure 5: Typical amplitudes and frequencies of biomagnetic signals and some noise sources.

The control EF or MF signal is applied to FE or FEM crystal by CPC or polar plates respectively. At the same time, these quantities are present in the ambient EM field and are generated under natural oscillations of the body surface (Fig. 5). In Earth DC MF, these quantities are present with the CPCs attached to the body surface. That is why the control and spurious signals are summarizing in a spontaneous manner. In such case, an analytical description of the introduced interferences is necessary for determination of the noise level of the invented magnetic amplifier [4].

In a general case, the output e. g. f. of PC, which is referring to one turn of its winding, is defined by the equation:

$$e=\frac{-d}{dt}[B_0 S_{eqv}\cos(\alpha_1(t))+B(t)\cdot S_{eqv}\cdot\cos(\alpha_2(t))] \quad (11)$$

where B(t)- a modulus of the AC MF induction vector; B_0- a modulus of the DC MF induction vector; $\alpha_1(t)$, $\alpha_2(t)$- are the angles between a magnetic axis of IC and vectors of B(t) and B_0 respectively; S_{eqv}- an equivalent square of PC.

The value of a corresponding signal-to-noise n_{sn} is expediently to define upon the different relationships between ω (measuring signal B) and Ω (interference from the unwanted oscillations):

1) when $\omega>>\Omega$ the output signal of EMTM according to Eq. (11):

$e_1'\approx A_0\cdot\sin\omega t+ A_0\cdot\Delta\alpha_2\cdot tg\,\alpha_2\cdot\cos\omega t$ and

$$n_{sn}'=2/\Delta\alpha_2\cdot tg\,\alpha_2; \quad (12)$$

2) if the frequency of a valid signal is equal to an interference's one ($\omega=\Omega$):

$e_1''\approx A_0\cdot\sin\omega t+ A_0\cdot\Delta\alpha_2\cdot tg\,\alpha_2\cdot\cos 2\Omega t$ and

$$n_{sn}''=1/\Delta\alpha_2\cdot tg\,\alpha_2 \quad (13)$$

in a twice frequency of a valid signal.

Taking into account the predominance of infra- and LF partials in interference's spectrum, advantageously to include into transducing circuit the high-order n-filters of HF. Than a factor of suppression the interferences k_{supp} can be presented as:

$$k_{supp}=\left(1-\frac{2\delta_f}{n}\Omega_{norm}^2\right)^{n/2} \quad (14)$$

where $\Omega_{norm}=\omega_{LF}/\omega$ is a normalized frequency of suppression; ω_{LF}- lower cut-off frequence of EMTM.

3 ENERGY-EFFICIENT AREA OF PC

Coverage can be achieved by designing some kind of density control mechanism, that is, scheduling the sensors to work alternatively to minimize the power wastage due to the overlap of active nodes' sensing areas [5]. The sensing area of a node is a disk of a given radius (sensing range). The sensing energy consumption is proportional to the area of sensing disks by a factor of μ_1, or the power consumption per unit. Then, the sensing energy consumption per (unit) area (SECPA) is $E = \mu_1\cdot D$, and for model we have:

$$E=\mu_1(\pi/2)\approx 1.57\,\mu_1 \quad (15)$$

If every four equal neighboring disks in model are tangent, then there is a gap between them (see Fig. 6). That uncovered space may be covered by one extra disk.

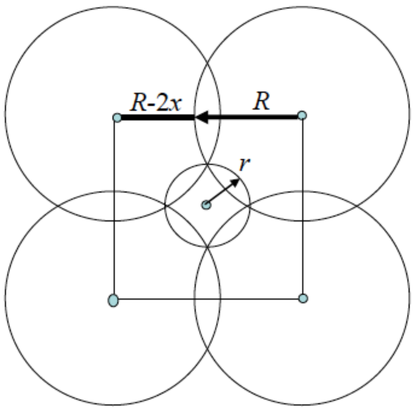

Figure 6. Optimal arrangement of sensors with two adjustable sensing ranges.

If the energy consumption of a disk of radius r is proportional to r^2, $n\geq 2$, then one could save energy by decreasing the radius of an extra disk. In order to decrease the radius r of an extra disk and to preserve the coverage, the neighboring disks of radius R must overlap. Though this overlapping may be small, the radius r may decrease gradually. We seek an optimal radius r for the extra disk, and this determines the extent to which the disks of radius R overlap. This case is intermediate between the previous models, and we will illustrate its advantage over them.

The tile is a square with vertices in the centers of four neighboring disks of radius R (see Fig. 6). Note that in that case, the diagonal disks do not intersect, but all these four disks are the neighbors of an extra disk of radius r.

As a result, we have the ratio of the total area $Sf=6\pi R^2/5$ of the parts of disks inside the tile divided by the area $Sp=16R^2/5$ of the tile, and the coverage density $D=3\pi/8\approx 1788$, and $E\approx 1.178\mu_1$. The sensing energy consumption is proportional to the area of sensing disks, or the power consumption per unit.

A fine structure of a sheathing network makes it possible to investigate the microstructure of the biomagnetic field. This innovation gives direction to the further investigation of nanowires and CNT in the direction of improving their conductivity and flexibility.

4 RESULTS

Simultaneous amplification of the piking up MCG&MEG neurosignals by an on-site magnetic flow has been implemented. Matrix of the sensing micro-nanoPCs are distributed under the heart or brain surface with temperature of the body. MF interferences from the breathing and heart-beating oscillations are filtered. Energy efficient area coverage of the advanced EM amplifier is expressed in terms of a disk of a given radius (sensing range).

The explained SV are calculated for the different CPC lengths on an order of 2 cm with a diameter of wire 0.1mm:

SV \ k_2	200	400	600	800	1000
M_W, H	13.2	11.46	10.95	10.7	10.6
C_M, pF	0.9	1.9	3	4.1	5.2

Table 1: The dependences of SV from a number of coil turns.

The relationship (14) is laid down as a basis for calculation of the dependences, that are shown in Fig. 7. The graphs can serve as recommendations for choosing the necessary order n of HF filter, dependently on the necessary value of k_{supp} under the different values of Ω_{supp} and Ω=1 Hz.

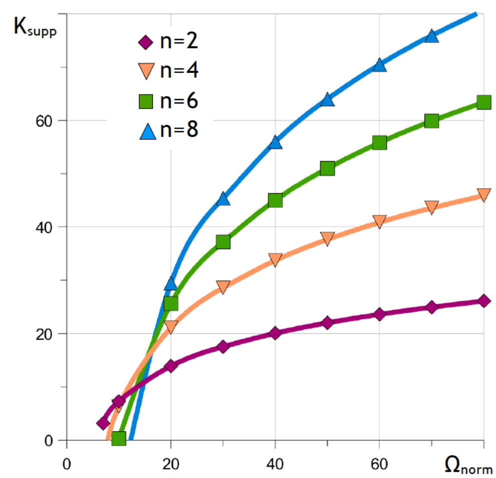

Figure 7: The relationship between a suppression factor of HF filter and chosen cut-off frequency for a different filter powers **n**.

REFERENCES

[1] V. Leonov, T. Torfs, Ch. V. Hoof and R. J. Vullers, Sens. & Transd. J., 107, pp. 165-176, 2009.

[2] Chen and Bai, "Proceedings of ICME International Conference on Complex Medical Engineering", 9-11April 2009, Tempe, AZ, USA, 1-5, 2009.

[3] Sklyar, "Nanotech 2008: Life Sciences, Medicine, and Bio Materials", Nano Science & Technology Institute, Cambridge, MA, USA, CRC Press, vol. 2, chapt. 6: NanoMedicine & Neurology, pp. 475-478.

[4] Sklyar, "Proceedings of 6th International Conference on Biomedical Applications of Nanotechnology", 4-6 March 2009, Charite, Berlin, Germany, 2 pages, 2009.

[5] V. Zalyubovskiy, A. Erzin, S. Astrakov and H. Choo, Sensors, vol. 9, pp. 2446-2460, 2009.